Supplemental Information

NO-to-NO_2 Conversion Rate Analysis and Implications for Dispersion Model Chemistry Methods using Las Vegas, Nevada Near-Road Field Measurements

Sue Kimbrough[1], R. Chris Owen[2], Jennifer Richmond-Bryant[3], Michelle Snyder[4]

[1]*U.S. Environmental Protection Agency, Office of Research and Development, National Risk Management Research Laboratory, 109 TW Alexander Dr., RTP, NC 27711*
[2]*U.S. Environmental Protection Agency, Office of Air Quality Planning and Standards, 109 TW Alexander Dr., RTP, NC 27711*
[3]*U.S. Environmental Protection Agency, Office of Research and Development, National Center for Environmental Assessment, 109 TW Alexander Dr., RTP, NC 27711*
[4]*University of North Carolina, Institute for the Environment, Center for Environmental Modeling for Policy Development, 100 Europa Dr., Chapel Hill, NC 27517*

1. Introduction – Supplemental Information

The basis for this research study was a legal challenge brought by the Sierra Club in 2002 over the adequacy of the Nevada Department of Transportation's (DOT's) National Environmental Policy Act assessment documentation developed for the widening of US 95, a major highway running through Las Vegas, NV. The resolution of this legal challenge was a settlement agreement between the Federal Highway Administration (FHWA), Nevada DOT and the Sierra Club. An element of this settlement agreement was a research study that would characterize the impact and behavior of particulate matter with aerodynamic diameter less than 2.5 μm and mobile source air toxics near highways (Kimbrough et al., 2008). The field study was conducted in Las Vegas, Nevada (NV), from mid-December, 2008, thru mid-December, 2009.

2. Measurements

2.1. Field campaign, analytical instruments, measurements

Four air measurement stations were located in the vicinity of I-15, approximately 1,430 m north of the I-15 interchange and approximately 1,070 m south of the Russell Road interchange. Three of the four stations were situated east of I-15, downwind of the freeway approximately 20 m, 100 m, and 300 m distant. One station was situated west of I-15, upwind of the freeway and approximately 100 m distant. A map of these measurement stations is shown in **Fig. S1** (Kimbrough et al., 2013b).

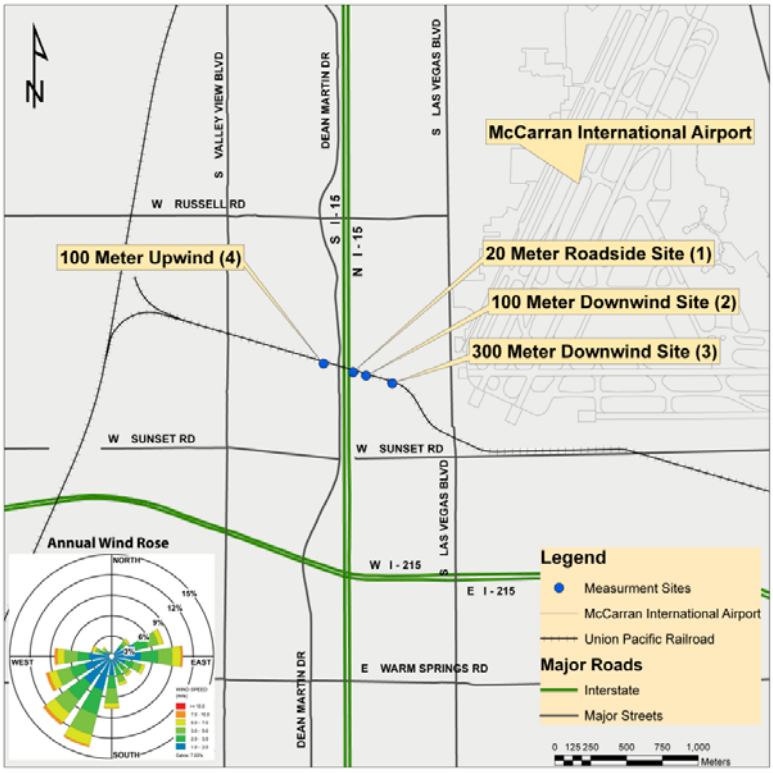

Fig. S1. Las Vegas, Nevada, Field Site with pollutant measurement locations at 20, 100, and 300 meters to the east of southbound I-15 and one location 100 meters to the west of southbound I-15. Annual wind rose shown at bottom left (Kimbrough et al., 2013b).

Ecotech model 9841T continuous gas analyzers (Ecotech Pty. Ltd., Knoxfield, Victoria, Australia) continuously streamed 5-minute data, and WinAQMS/WinCollect software (Ecotech Pty. Ltd., Knoxfield, Victoria, Australia) logged the data (Kimbrough et al., 2013a; Kimbrough et al., 2013b). The continuous gas analyzers were set up to run nightly zero and span points. These analyzer checks typically ran between the hours of midnight and 2 am every day during the course of the study. As a consequence, the study has substantially fewer 5-minute data points for these hours. These hours were chosen for the nightly zero and span points as the study design protocol called for the instrumentation to be operational during peak traffic conditions (FHWA, 2006).

Table S1. Summary of measurements discussed herein (Kimbrough et al., 2013a; Kimbrough et al., 2013b).

Measurement Parameter	Distance from I-15 (m)				Sampling Approach	Instrument Data				
	Upwind	Downwind				Make/Model	Accuracy	Precision	Detection Limit	Sample Type and Frequency
	100	20	100	300						
Oxides of nitrogen (NO_x)	X	X	X	X	Chemi-luminescence	EC 9841B	< 1%	0.5 ppb	0.5 ppb	Continuous (5 minutes)
Wind Speed	X	X	X	X	Sonic anemometer	RM Young Model 81000	±0.05 m/s	std. dev. 0.05 m/s at 12 m/s	0.01 m/s	Continuous (5 minutes)
Wind Direction	X	X	X	X	Sonic anemometer	RM Young Model 81000	± 5°	± 10°	0.1°	Continuous (5 minutes)
Meteorological tower height above ground level (m) -- includes shelter height: 11.8							N/A			---
Traffic (vehicle counts, speed)	Data provided by Nevada DOT				Radar	Radar (Wavetronix)	N/A			Continuous (15 minutes)

Las Vegas is located at approximately 665 m above sea level and surrounded by mountains on all sides. The surrounding mountains have elevations ranging from 1000 to 2000 m higher than the city's elevation. As a result of this complex topography, complex meteorological conditions are a feature of this area. Winds are typically from the southwest, although there are

seasonal variations–during the winter season, northern winds predominate (Kimbrough et al., 2013b).

Urban field study locations can be problematic due to the needs of the research study, topography, administrative barriers, technical issues, etc., and this study was no exception. Study design issues included: 1) a depressed section of freeway; 2) an adjacent Union Pacific Railroad (UPRR) spur line; 3) a nearby parking lot; 4) the proximity to Las Vegas Boulevard McCarran International Airport; and 5) the time-of-day of the calibrations for the continuous gas analyzers (i.e., nightly zero-spans).

As described in Baldauf et al. (2013), the depressed section of freeway crosses under a spur of the UPRR by approximately 5 m. Data analysis indicated that pollutant concentrations were impacted only during calm-to-light variable wind conditions (Baldauf et al., 2013).

The usage of the UPRR spur line is typically limited to one train run a day from Las Vegas, NV, to Henderson, NV, in the morning, returning in the afternoon to Las Vegas, NV. Since the influence of the passage of the train was a concern, a video camera with date and time stamp information was used to correlate with the collection of the 5-minute continuous data [carbon monoxide (CO), NO_X, and black carbon (BC)]. When observing the second-by-second data from the continuous analyzer, field site operators noted impacts from the train. However, an analysis of the 5-minute data during the passage of the train revealed that there were no detectable impacts from the train.

A nearby parking lot, used as a staging area for Las Vegas Convention Center truck deliveries, may have impacted air pollutant concentrations. Trucks utilized this parking lot on a variable schedule with trucks remaining in the parking lot for multiple days at a time. The

influence on measurements, if any, would be highly variable due to the unpredictable nature of the truck schedules and had not been able to be fully characterized by previous analyses of the data.

The 300 m downwind site was approximately 200 m west of Las Vegas Boulevard and 430 m west of the fence line of the Las Vegas McCarran International Airport. Las Vegas Boulevard, historically a major artery through the city but now a city street serving tourist and local traffic, supported approximately 50,000 vehicles/day during the study. In the case of either Las Vegas Boulevard or McCarran International Airport, measurements would likely only be impacted when winds were from the east.

2.2. Ozone Measurements

There were no collocated ozone measurements taken at the field study site. However, ozone concentration is valuable to study the chemical transition of NO emissions to NO_2. Measurements of ozone were taken in the Las Vegas area, both north of the I-15 field study site (these locations are shown in Fig. S2). The locations of the ozone monitors are both north of the I-15 field site, one east, Orr, and one west, Paul Meyer, of I-15 which runs north-south. These measurement locations are located significantly further away from I-15 than any of the field measurement locations, so they are influenced by other urban factors. However, as shown in Fig. 1, they have a similar temporal pattern, and thus are representative of the background ozone level.

Fig. S2. Locations of ozone monitors near the Las Vegas field site by the yellow markers. The Las Vegas field site is indicated by the red marker.

2.3. Traffic Data, Vehicle Fleet Mix and NO_X Emissions

Nationally, the estimated 2008 National Emissions Inventory (NEI) contribution of highway vehicle NO_X emissions to the total anthropogenic NO_X emissions was approximately 39% (Table S2). The contribution of NO_X emissions from heavy-duty diesel vehicles was approximately 17% (U.S. EPA, 2008). The relatively high emissions contribution from heavy-duty diesel vehicles is due to high engine emission rates and vehicle miles traveled (Huai et al., 2006). The contribution of mobile source NO_X emissions to anthropogenic total NO_X emissions varies from area to area based on the relative contributions from other anthropogenic sources such as stationary fuel combustion (U.S. EPA, 2008).

Based on traffic count information received from the Nevada Regional Transporation Commission (RTC), the annual average daily traffic (AADT) for the I-15 site was approximately 161,500 (mid-December 2008 – mid-December 2009). Vehicle fleet estimates prepared by

Environ International Corp. (2007) for Clark County, NV, which includes the Las Vegas, NV, urban area (96% light-duty vehicles; 4% heavy-duty vehicles) is similar to the fleet mix estimate derived from actual traffic volume data reported by Nevada RTC (95% light-duty vehicles; 5% heavy-duty vehicles). The light-duty vehicle classification includes passenger cars, light trucks [< 8,500 pounds (lb) gross vehicle weight rating (GVWR)] and motorcycles. The heavy-duty truck classification includes heavy-duty single-unit trucks and articulated trucks > 8,501 lb GVWR and heavy-duty buses (including school buses and transit buses).

The total on-road NO_X emissions (2008 NEI) for Clark County, NV, was approximately 19 x 10^3 short tons per year. The contribution by on-road gasoline vehicles was 13 x 10^3 short tons per year (68% of the total on-road emissions). The contribution by on-road diesel vehicles was 6 x 10^3 short tons per year (approximately 32% of the total on-road emissions).

A review of data from EPA's Where You Live web page (http://www.epa.gov/air/emissions/where.htm , last accessed October, 2016) provided an indication of local major NO_X emission sources (i.e., electric utility combustion sources). The nearest electric utility combustion source in the nearby Las Vegas, NV, area was more than 11 kilometers east of the monitoring stations. Under downwind condtions (winds from west), NO_X emissions from this electric utility combustion source would not influence NO_X measurements. We also reviewed the locations of major NO_X emission sources in California and found the closest electric utility combustion source of NO_X emissions to be more than 200 kilometers southwest of the monitoring stations. This source emitted less than 0.6 short tons per day. Based on these locations, these non-motorized sources of NO_X likely contributed only to background concentrations, which were estimated by the upwind monitoring station.

Table S2. Clark County (Las Vegas) traffic volume, vehicle fleet mix and NO_X emissions.

Annual Average Daily Traffic (AADT) for I-15 Site		161,500	
Vehicle Classification	**Fleet Mix (%)** **(Environ International Corp., 2007)**	**Nevada RTC Traffic Data**	
		Traffic Volume **(AADT)**	**Fleet Mix (%) Based on Traffic Volume Vehicle Length Bins**
Light-duty vehicles	96	155,360	95
Heavy-duty vehicles	4	6,140	5
	2008 National Emissions Inventory (%) **(U.S. EPA, 2008)**	**NO_X Emssions (tons per year)**	
On-road gasoline vehicles	68	13×10^3	
On-road diesel vehicles	32	6×10^3	

3. Results and Discussion

The near-road downwind measurement locations were strategically located to the east of the roadway, thus we subset the data to only look at when the winds were blowing from the west in a 120-degree sector centered at the normal to I-15. These winds were further subset to only include hours when the measured NOx decreased or stayed the same as the plume moved from the roadway to the measurement locations (called "Q3", more explanation may be found in Section 3.2). The total dataset, winds from the west, and the Q3 subsets are summarized in **Table S3**. The total hours for each dataset are shown with percentages of the total hours in the full dataset. Number of hours and percentages by season, day of week, and ozone are calculated from the subset total.

Table S3. Measurement dataset and subsets summaries for all data and two subsets.

Dataset:	**All Data**	**From West**	**From West & in Q3**
Total	6849 (100%)	2668 (39.0%)	2178 (31.8%)
Season			
Spring	1800 (26.28%)	722 (27.06%)	584 (26.81%)
Summer	1693 (24.72%)	612 (22.94%)	534 (24.52%)
Fall	1447 (21.13%)	527 (19.75%)	433 (19.88%)
Winter	1909 (27.87%)	807 (30.25%)	627 (28.79%)
Day of Week			
Weekday	4938 (72.10%)	1943 (72.83%)	1563 (71.76%)
Weekend	1911 (27.91%)	725 (27.17%)	615 (28.24%)
Ozone			
High (> 30ppb)	3758 (54.87%)	1080 (40.48%)	966 (44.35%)
Low (<= 30 ppb)	3091 (45.13%)	1588 (59.52%)	1212 (55.65%)
	ppb	ppb	ppb
Max	82.00	73.00	73.00
75^{th} percentile	47.50	44.00	45.75
Median	33.00	22.00	25.00
Mean	31.52	25.51	27.71
25^{th} percentile	14.50	6.00	8.00
Min	0.00	0.00	0.00
Hourly Traffic			
	Number of Vehicles	Number of Vehicles	Number of Vehicles
Max	12090	11880	11690
75^{th} percentile	9252	8126	8364
Median	7185	5776	6151
Mean	6859	6004	6238
25^{th} percentile	4586	3598	3829
Min	161	469	469

3.1. Spatial Gradient Results

The percentile of the hourly measured NO_2/NO_x ratio at each of the four measurement locations is presented in **Fig. S3.** The only downwind monitoring location with a total conversion of NO to NO_2 is the 300 m site, and less than 1% of the hours have > 0.99 NO_2/NO_X conversion. Thus, the assumption of total conversion is not applicable within 300 meters of a major roadway.

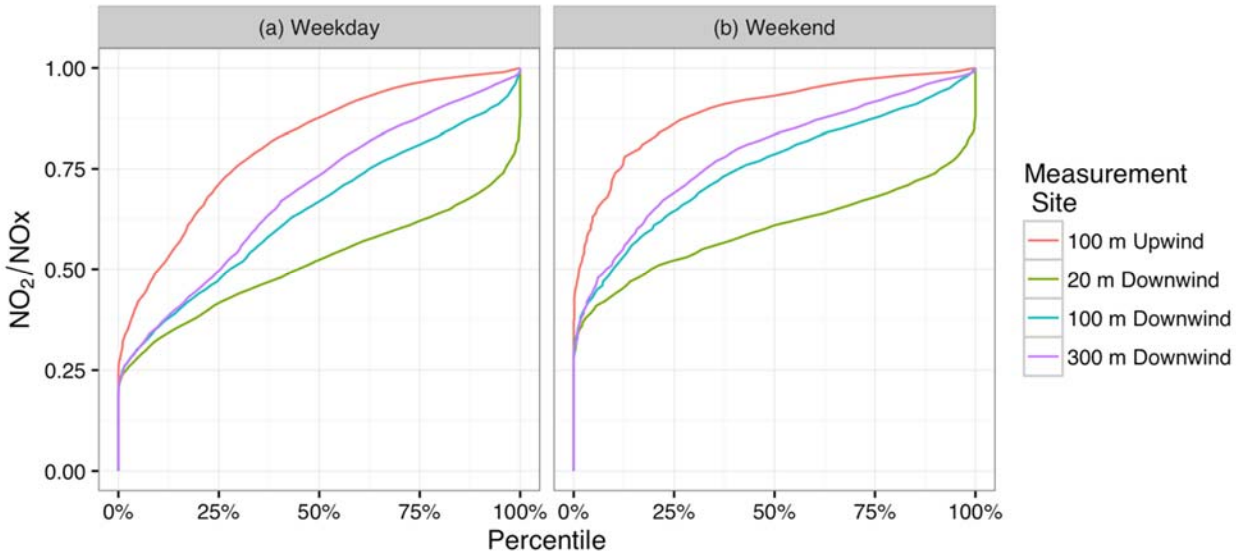

Fig. S3. Percentile of NO to NO_2 conversion rates for: (a) weekday, and (b) weekend hours. Measured NO_2/NO_X ratio for: (a) weekday, and (b) weekend for all sites when winds are from the west.

To further examine the diurnal pattern in measured NO_2 concentrations between measurement sites, **Fig. S4** is presented. The diurnal pattern on weekends and weekdays are similar at all locations. However, there is a clear magnitude difference in the morning transition hours, between 5 am and 7 am. This magnitude difference is due to the difference in the fleet mix

on weekends vs. weekdays, when there is a higher traffic count and higher percentage of light-duty vehicles (i.e., cars) on weekdays (see **Fig. S1**).

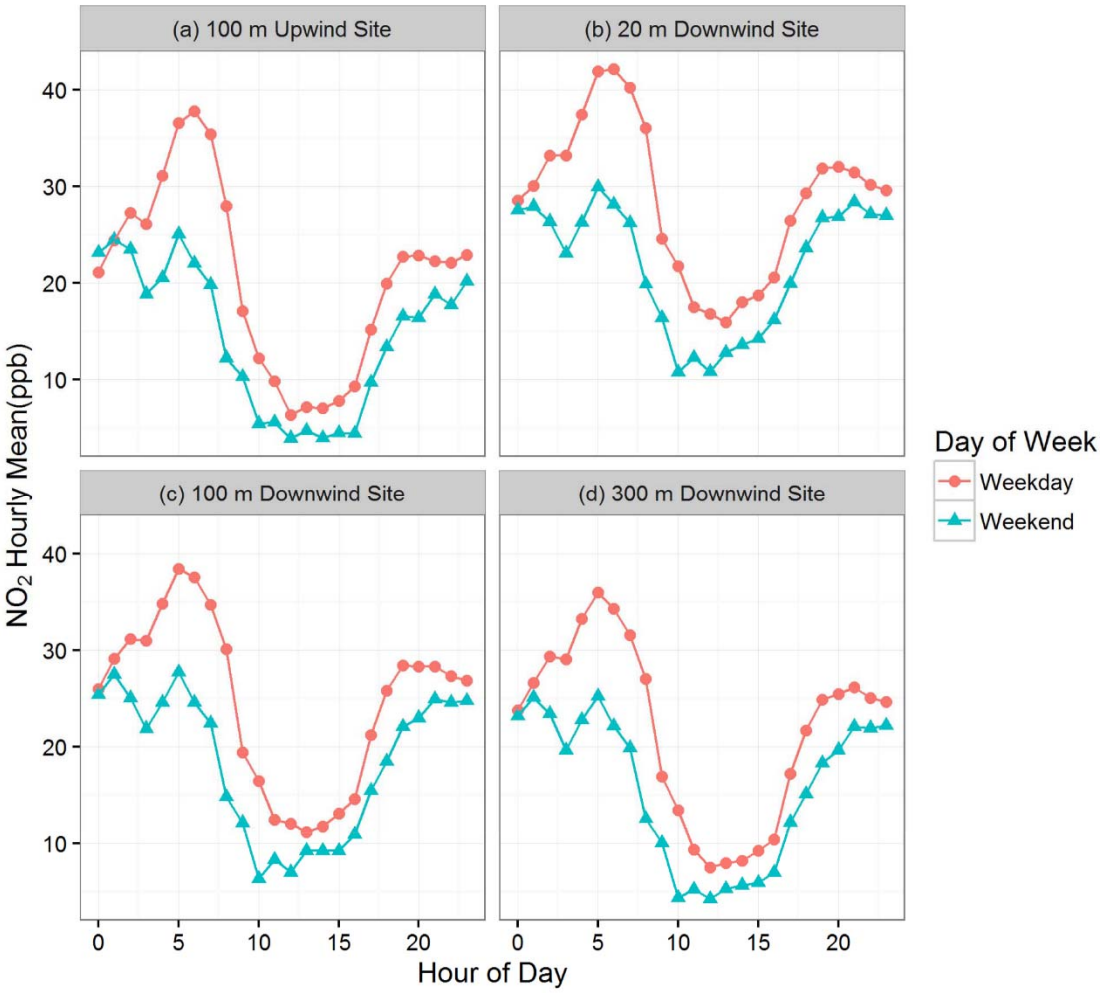

Figure S4. Hourly mean NO_2 concentration at all measurement sites, downwind conditions: (a) -100 m upwind. (b) 20 m roadside. (c) 100 m downwind. (d) 300 m downwind when winds are from the west.

3.2. Change in NO_X between measurement sites

As has been documented by previous work (Kimbrough et al. 2013), there are some measurements that are influenced by NO_x sources other than the roadway (also discussed above, in Section 2.1). We present **Fig. S5** to examine the trends in NO_x measured at consecutive downwind measurement locations. **Fig. S5** shows the change in total measured NO_x between the

20 m and 100 m sites versus the change between 100 m and 300 m measurement locations, shaded to show the measured ozone. We examined the weekday and weekend changes in NO_X between the sites, focusing on two cases: 1) an increase in total measured NO_X between the 100 and 300 m measurement locations, but a decrease in total measured NO_X between the 20 and 100 m measurement locations relative to the 100 m upwind site (Quadrant 2); 2) an increase in total measured NO_X between the 20 and 100 m measurement locations and a decrease in total measured NO_X between the 100 and 300 m measurement locations relative to the 100 m upwind site (Quadrant 4). These two cases seem impossible without a source of NO_X located between the measurement sites. After determining that these were erroneous measurements, possibly due to nearby sources of NO_X, further analysis was limited to data points showing that the difference in total measured NO_X decreased from the 20 m to the 100 m to the 300 m sites, as one might expect from dilution with background air (Quadrant 3). Only data that meet the criteria of Quadrant 3 were used in the analysis.

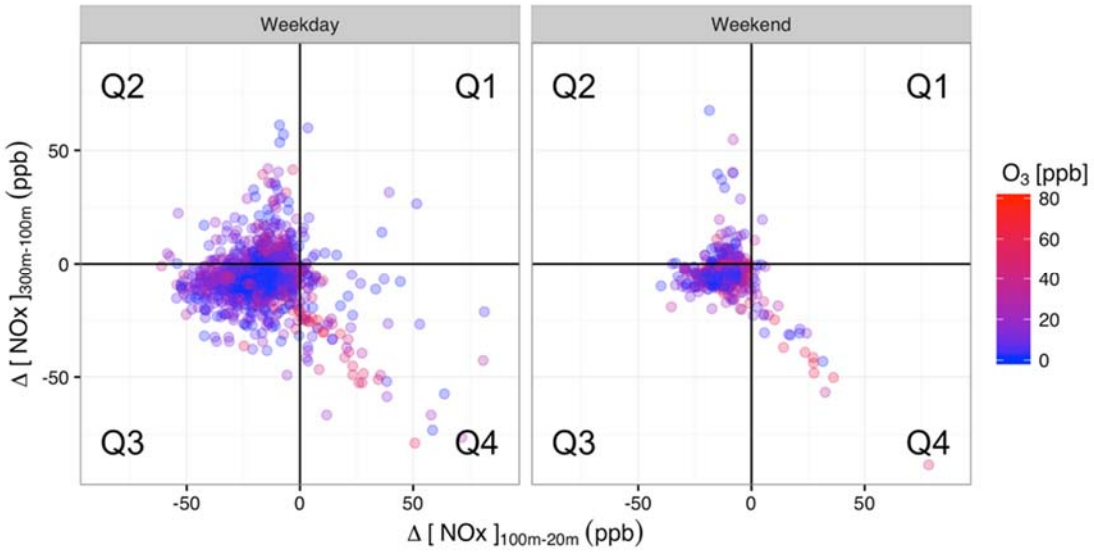

Fig. S5. Hourly change in NO_X between the three downwind measurement sites when the winds are from the west. Shading is a function of the measured ozone. Data are separated into weekday (left-hand panel) and weekend (right-hand panel) hours where we have different ozone levels. Day is defined as 8 am to 8 pm, night is defined as 8 pm to 8 am.

3.3. NO_2/NOx ratio as a function of measured and calculated variables

We examined the pattern in the NO_2/NOx ratio and ozone as a function of wind speed, temperature, frictional surface velocity, traffic volume, mixing height, Monin-Obukhov length, and plume volume. In addition, we looked at the trends between mixing height and ozone during different time periods of the day.

First, we examined low ozone (≤ 30 ppb) conditions as a function of wind speed in **Fig. S6**, where the hourly ratio is colored by measured ozone. The majority of the wind speeds in these low ozone conditions are < 3 m/s. However, the range of the NO_2/NO_x ratio is between 0.25 and 1.0 without a trend relating wind speed and the ratio. A linear fit to the data is presented for each measurement location on the weekday and weekend. However, there is a very low r^2 value, indicative of data with weak or no fit.

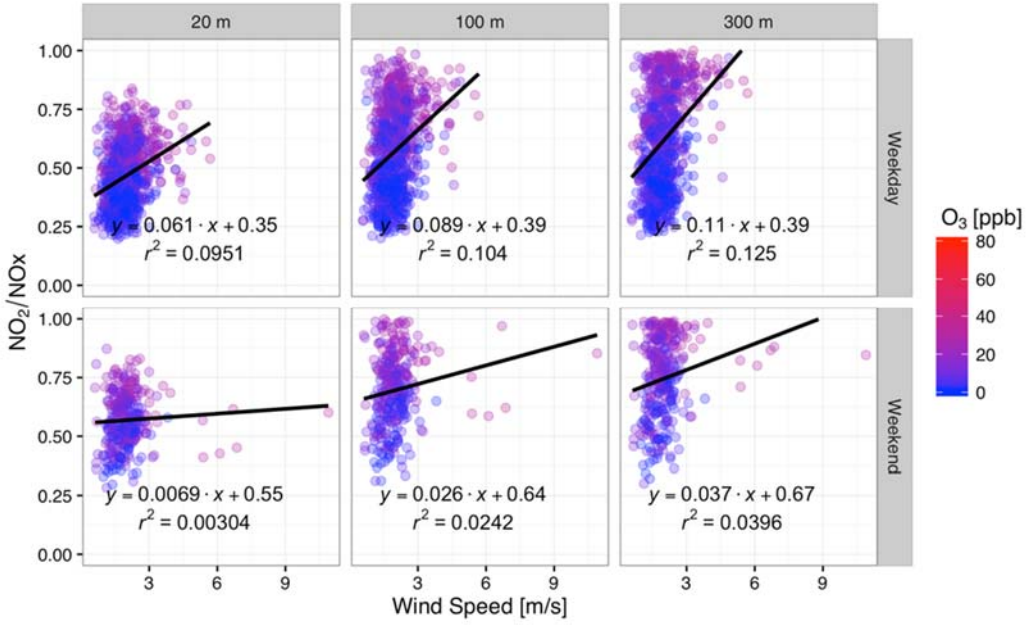

Fig. S6. NO_2/NO_x ratio as a function of wind speed is filled by ozone concentration, where only low ozone (≤ 30 ppb) conditions when winds are from the west and in Q3 are shown. Top row is weekdays; bottom row is weekends. Left-hand column shows the 20 meter measurement site, center column shows the 100 m measurement site, and the right-hand column shows the 300 m measurement site.

Next, we examine the NO_2/NOx ratio as a function of temperature under all ozone conditions in **Fig. S7**, shaded by the measured ozone. Here, there is no discernible pattern in the ratio as a function of temperature at any of the measurement locations. There is a notable pattern where high ozone typically occurs at higher temperatures, in agreement with the diurnal ozone pattern having a peak during the mid-day when the temperatures are typically higher. Otherwise, we see weak to no discernible trend in the NO_2/NOx ratio as a function of temperature.

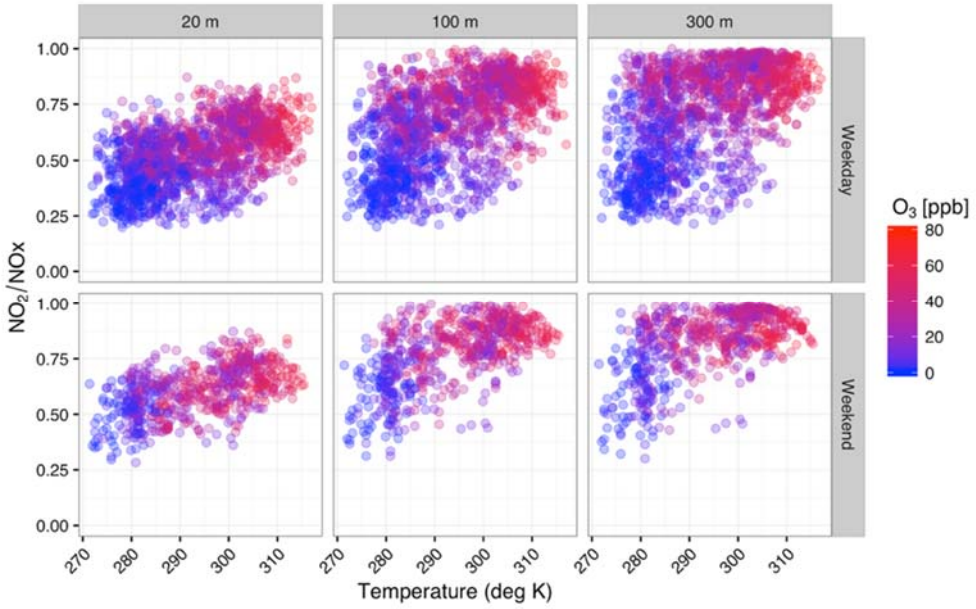

Fig. S7. NO_2/NO_x ratio as a function of measured temperature when winds are from the west and in Q3. Points are filled by ozone concentration, where all ozone conditions are shown. Top row is weekdays; bottom row is weekends. Left-hand column shows the 20 meter measurement site, center column shows the 100 m measurement site, and the right-hand column shows the 300 m measurement site.

We examine the NO_2/NO_x ratio as a function of the surface frictional velocity, u*, under all ozone conditions in **Fig. S8**, shaded by the measured ozone. Here, there is a slight pattern under higher ozone conditions where the ratio decreases as a function of u*. This pattern is somewhat expected, since there is a similar pattern with wind speed under high ozone conditions, and u* is a function of wind speed (see Cimorelli et al., 2005). For low ozone conditions, there is

not a pattern, again (as expected) similar to the analysis in **Fig. S6**, where there is weak to no pattern in the NO_2/NO_x ratio as a function of wind speed. For high ozone conditions, there is a slight negative trend in the NO2/NOx ratio as u*increases, but there is a stronger relationship with the first-order wind speed, as shown in **Fig. S6**.

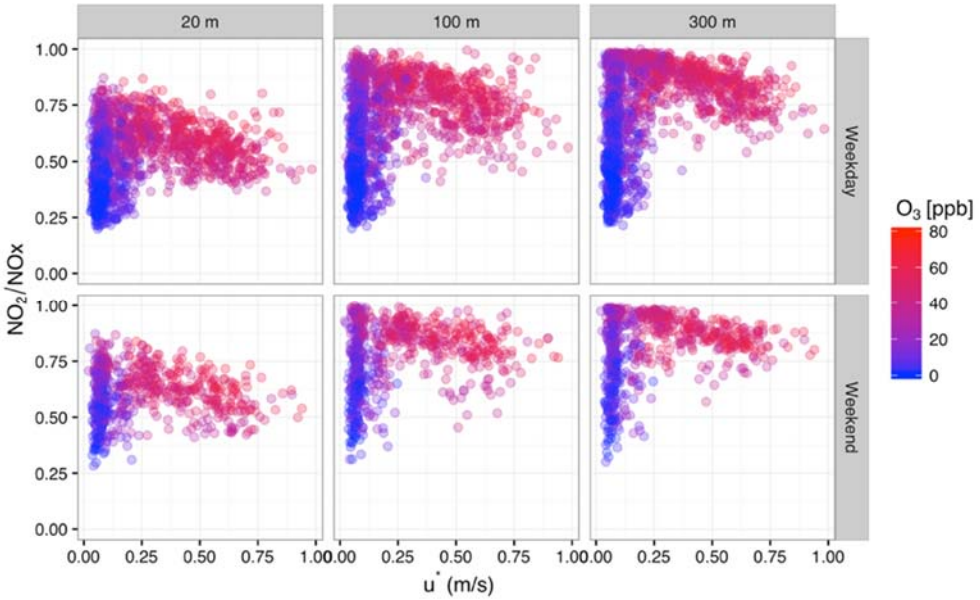

Fig. S8. NO_2/NO_x ratio as a function of the surface frictional velocity, u^*, at each measurement location when winds are from the west and in Q3. Points are filled by ozone concentration, where all ozone conditions are shown. Top row is weekdays; bottom row is weekends. Left-hand column shows the 20 meter measurement site, center column shows the 100 m measurement site, and the right-hand columns shows the 300 m measurement site.

The NO2/NOx ratio as a function of the measured traffic volume under all ozone conditions is shown in **Fig. S9**, shaded by the measured ozone. Measured traffic volume is used as a surrogate for the amount of emissions on the roadway. Here, there is no discernible pattern under any ozone conditions or as a function of traffic volume.

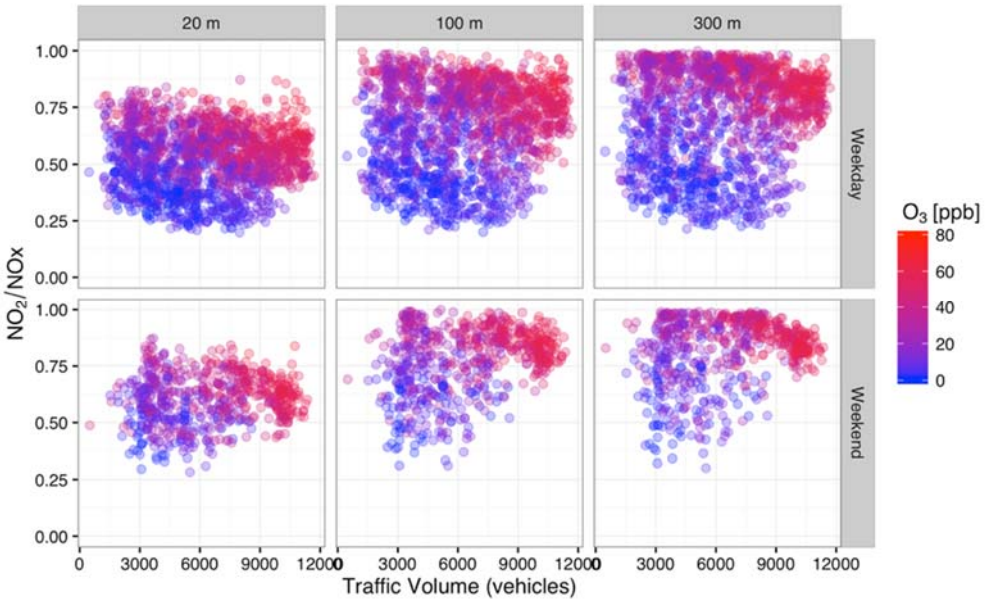

Fig. S9. NO_2/NO_x ratio as a function of measured traffic volume at each measurement location when winds are from the west and in Q3. Points are filled by ozone concentration, where all ozone conditions are shown. Top row is weekdays; bottom row is weekends. Left-hand column shows the 20 meter measurement site, center column shows the 100 m measurement site, and the right-hand column shows the 300 m measurement site.

The NO_2/NOx ratio as a function of the mixing height under all ozone conditions is shown in **Fig. S10**, shaded by the measured ozone. We notice that the low ozone conditions are seen when the mixing height is low, indicative of stable conditions of the overnight hours when ozone levels are low (**Fig. S2**). The higher ozone conditions occur when mixing heights are higher, from 500 to 4000 meters. Higher mixing heights are indicative of convective conditions, which occur during the daytime hours when there are high ozone levels (**Fig. S2**). The NO_2/NO_x ratio varies between 0.25 and 1.00 for all mixing heights between 500 meters and 4000 meters, with weak to no pattern.

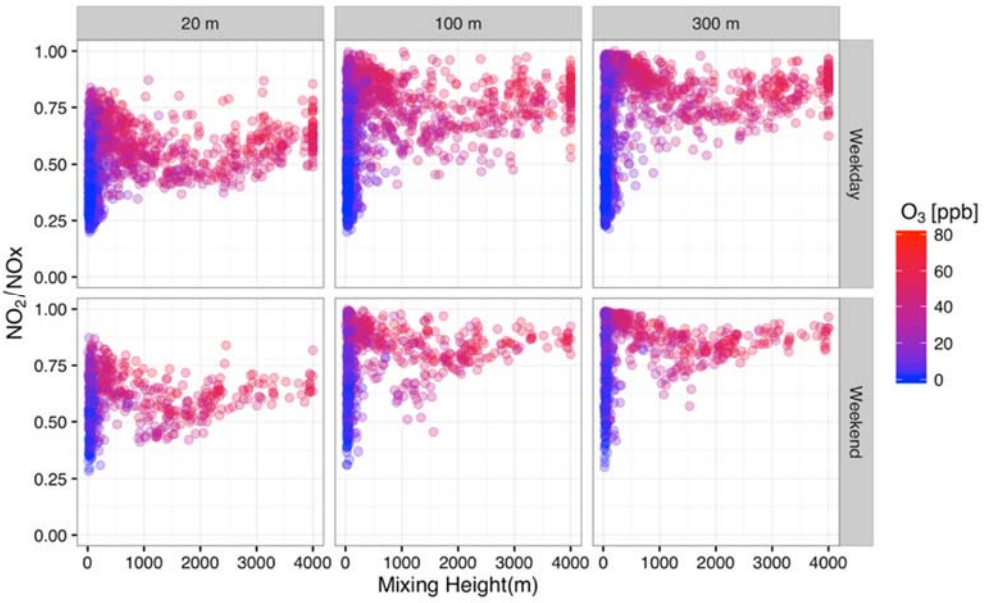

Fig. S10. NO_2/NO_x ratio as a function of the mixing height. Points are filled by ozone concentration when winds are from the west and in Q3, where all ozone conditions are shown. Top row is weekdays; bottom row is weekends. Left-hand column shows the 20 meter measurement site, center column shows the 100 m measurement site, and the right-hand column shows the 300 m measurement site.

The NO_2/NOx ratio as a function of the inverse of Monin-Obukhov length, a measure of atmospheric stability under all ozone conditions, is shown in **Fig. S11**, shaded by the measured ozone. We analyzed the inverse of the Monin-Obukhov length to avoid the discontinuity at zero, making a continuous scale of atmospheric stability. With this scale, negative values mean convective conditions, the larger in magnitude the more convective the conditions. Similarly, positive values on this scale indicate stable conditions, the greater the magnitude the more stable the atmosphere. Neutral conditions would be shown near 0. Again, as in **Fig. S10** and **Fig. S7**, there are lower ozone levels under stable conditions when temperatures and mixing heights are low. Likewise, higher ozone levels occur under convective conditions when there are higher temperatures and mixing heights. However, in terms of NO_2/NO_x ratio, there is no pattern with respect to the Monin-Obukhov length.

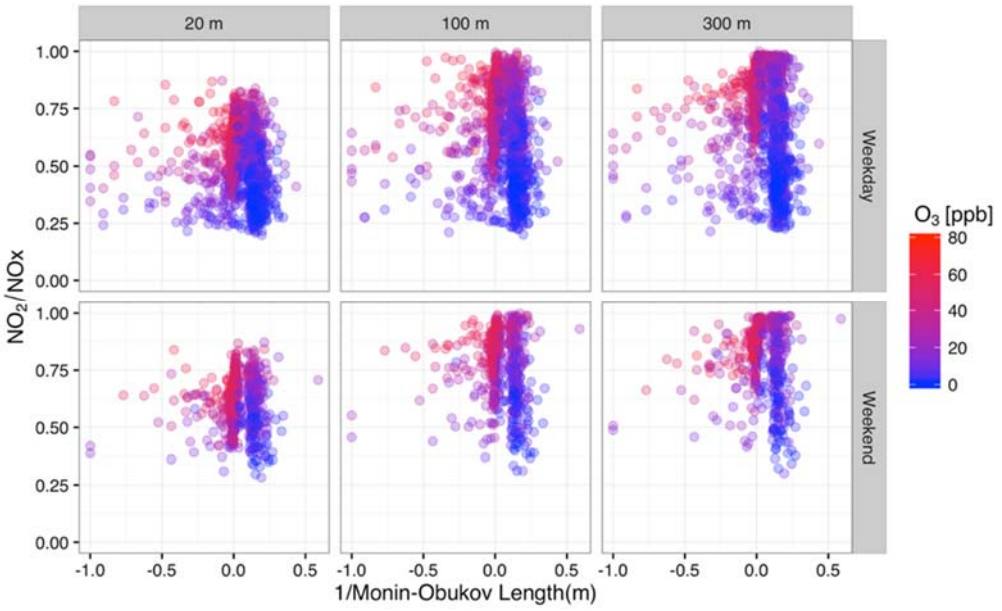

Fig. S11. NO_2/NO_x ratio as a function of the calculated Monin-Obukhov length inverse. Points are filled by ozone concentration when winds are from the west and in Q3, where all ozone conditions are shown. Top row is weekdays; bottom row is weekends. Left-hand column shows the 20 meter measurement site, center column shows the 100 m measurement site, and the right-hand column shows the 300 m measurement site.

Fig. S12 shows the NO_2/NOx ratio as a function of the plume volume, shaded by the measured ozone. The plume volume was calculated using the PVMRM method (Hanrahan, 1999) with approximations of vertical and horizontal spread used in AERMOD (Cimorelli et al., 2005) . Notice that the larger plume volumes tend to have larger NO_2/NO_x ratios. This is not surprising, since larger vertical and horizontal spreads occur under convective conditions, when the temperature, mixing height, and ozone are larger. Similarly, when the plume volume is < 25 m^3 the ozone levels under lower conditions are more stable, and temperatures and mixing heights are lower. Again, the trends are weak to non-existent with this derived parameter.

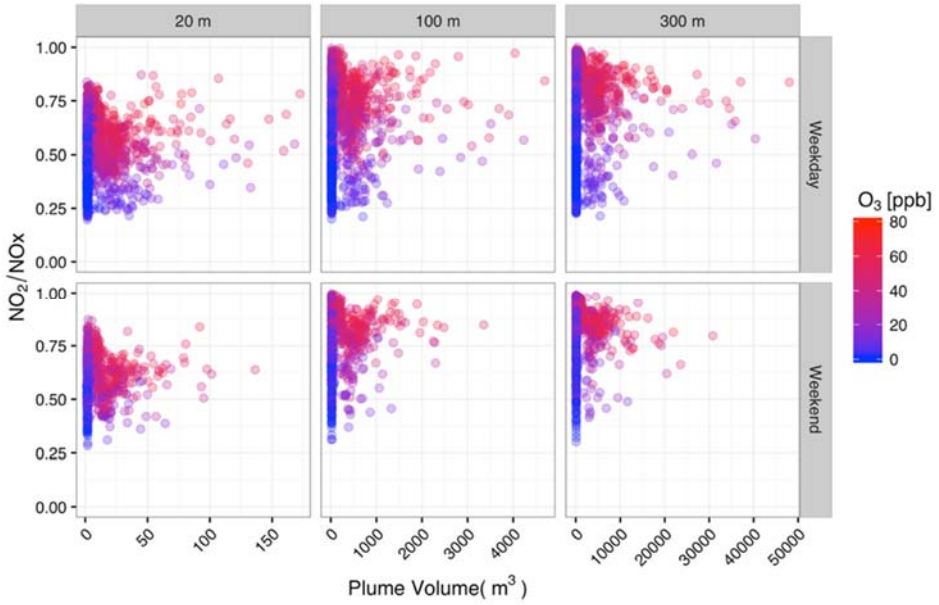

Fig. S12. NO_2/NO_x ratio as a function of NO_2/NO_x as measured at the estimated plume volume at each measurement location when winds are from the west and in Q3. Points are filled by ozone concentration, where all ozone conditions are shown. Top row is weekdays; bottom row is weekends. Left-hand column shows the 20 meter measurement site, center column shows the 100 m measurement site, and the right-hand column shows the 300 m measurement site.

As another analysis, we examined the pattern of mixing height versus measured ozone, shaded by time period of the day in **Fig. S13**. This figure highlights that the largest mixing heights occur in the daytime and evening hours when the ozone levels are higher. In addition, the lower mixing heights occur in the early morning and late evening. During these time periods, there is a large range in the measured ozone. During the morning transition hours, there is a mix of low to moderate ozone with low to moderate mixing heights, showing this period to be highly variable in atmospheric stability and NO to NO_2 conversion.

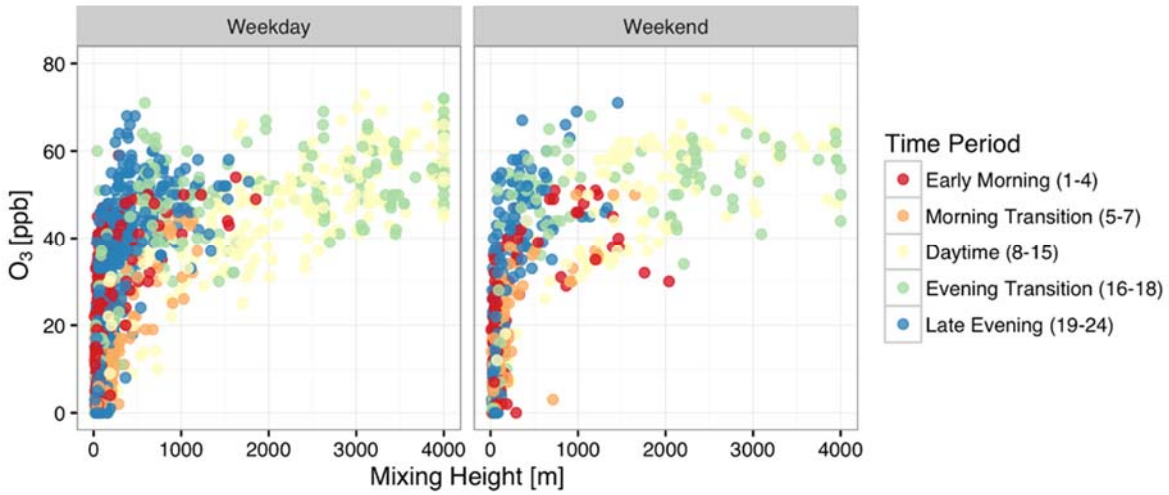

Fig. S13. Ozone as a function of the calculated mixing height when winds are from the west and in Q3. Points are filled by time of day. Left-hand plot shows weekdays; right-hand plot shows weekends.

The figures presented in this supplemental information are based on calculated boundary layer parameters and measured traffic volumes and temperatures. The trends in **Figs. S7**, **S10**, **S11, S12,** and **S13** highlight the interconnectedness of these meteorological parameters and calculated values. However, there are no significant trends between the NO_2/NO_x ratio and these parameters and the calculated values. In the main paper, we find that the strongest trends with the NO_2/NO_x ratio occur with the first-order parameter of wind speed and background NO_2/NO_x ratio under high ozone conditions, and only the background NO_2/NO_x ratio under low ozone conditions.

4. References

Baldauf, R.W., Heist, D., Isakov, V., Perry, S., Hagler, G.S.W., Kimbrough, S., Shores, R., Black, K., Brixey, L., 2013. Air quality variability near a highway in a complex urban environment. Atmospheric Environment 64, 169-178. http://dx.doi.org/10.1016/j.atmosenv.2012.09.054.

Cimorelli, A.J., Perry, S.G., Venkatram, A., Weil, J.C., Paine, R.J., Wilson, R.B., Lee, R.F., Peters, W.D., Brode, R.W., 2005. AERMOD: A dispersion model for industrial source applications. Part I: General model formulation and boundary layer characterization. Journal of Applied Meteorology 44, 682-693. http://dx.doi.org/10.1175/jam2227.1.

Environ International Corp., 2007. Clark County On-Road Mobile Source Emissions. Las Vegas, NV. http://www.clarkcountynv.gov/airquality/planning/Documents/SIP/ozone/App_A_Consolidated_Emissions_Inventory.pdf. Last Accessed: October 19, 2016.

FHWA, 2006. Detailed monitoring protocol for U.S. 95 settlement agreement. FHWA. Washington, DC, http://www.fhwa.dot.gov/environment/air_quality/air_toxics/research_and_analysis/near_road_study/finaldmpjune.pdf. Last Accessed: October 19, 2016.

Hanrahan, P.L., 1999. The Plume Volume Molar Ratio Method for determining NO_2/NO_X ratios in modeling - Part I: Methodology. Journal of the Air & Waste Management Association 49, 1324-1331. http://dx.doi.org/10.1080/10473289.1999.10463960.

Huai, T., Shah, S.D., Wayne, M., J., Younglove, T., Chernich, D.J., Ayala, A., 2006. Analysis of heavy-duty diesel truck activity and emissions data. Atmospheric Environment 40, 2333-2344. http://dx.doi.org/10.1016/j.atmosenv.2005.12.006.

Kimbrough, E.S., Baldauf, R.W., Watkins, N., 2013a. Seasonal and diurnal analysis of NO_2 concentrations from a long-duration study conducted in Las Vegas, Nevada. Journal of the Air & Waste Management Association 63, 934-942. http://dx.doi.org/10.1080/10962247.2013.795919.

Kimbrough, S., Baldauf, R., Hagler, G., Shores, R.C., Mitchell, W., Whitaker, D.A., Croghan, C.W., Vallero, D.A., 2013b. Long-term continuous measurement of near-road air pollution in Las Vegas: Seasonal variability in traffic emissions impact on local air quality. Air Quality, Atmosphere & Health 6, 295-305. http://dx.doi.org/10.1007/s11869-012-0171-x.

Kimbrough, S., Vallero, D., Shores, R., Vette, A., Black, K., Martinez, V., 2008. Multi-criteria decision analysis for the selection of a near road ambient air monitoring site for the measurement of mobile source air toxics. Transportation Research Part D: Transport and Environment 13, 505-515. http://dx.doi.org/http://dx.doi.org/10.1016/j.trd.2008.09.009.

U.S. EPA, 2008. National Emissions Inventory. https://www.epa.gov/air-emissions-inventories/2008-national-emissions-inventory-nei-data. Last Accessed: October 19, 2016.